

Thermal Chemistry of C₃ Allyl Groups on Pt(111)

Demetrius Chrysostomou and Francisco Zaera*

Department of Chemistry, University of California, Riverside, California 92521

Received: August 8, 2000; In Final Form: November 28, 2000

The thermal chemistry of allyl iodide and of allyl bromide adsorbed on Pt(111) was investigated by temperature-programmed desorption (TPD) and reflection–absorption infrared (RAIRS) spectroscopies. On the clean Pt(111) surface, both allyls were found to bond to the surface via the halogen atom in a gauche conformation and with the C–C–C plane close to parallel to the surface. In the presence of surface hydrogen, allyl iodide was found to tilt backward such that the C–C–C plane adopts a more vertical orientation on the surface; in this more upright geometry, both cis and gauche isomers were identified. With both molecules the facile thermally activated cleavage of the carbon–halogen bond results in the formation of C₃ allylic species on the surface. A η^1 allylic moiety was identified by RAIRS in the high-exposure regime of allyl iodide after annealing to 200 K, and the formation of a second η^3 allylic intermediate was inferred from TPD experiments with coadsorbed hydrogen and deuterium. At low surface concentrations, allyl moieties mainly dehydrogenate, ultimately to H_{2(g)} and C_{ads}. At coverages approaching monolayer, on the other hand, some of the allyls hydrogenate to propene around 310 K via a process which relies on the decomposition of a few of the same surface allyl moieties as the source of hydrogen. Hydrogenation to propene can be enhanced and induced at much lower temperatures by predosing hydrogen on the surface. This propene is seen to desorb in two temperature desorption peaks. The first, at 185 K, is likely to come from direct hydrogenation of the η^1 allyl intermediate, and does not involve any appreciable H–D exchange. The higher temperature desorption regime is observed around 250 K, and yields not only propene but also significant amounts of propane. In this case, a η^3 allylic species is believed to hydrogenate to di- σ bonded propene, and to subsequently undergo multiple propene–propyl–propene surface interconversions to produce extensive H–D exchanged products.

Introduction

The catalytic conversion of small-chain hydrocarbons by transition metal surfaces is of great relevance to the oil refining and petrochemical industries. The characterization of the reactivity of low molecular weight hydrocarbons with simple transition metal surfaces is a useful approach toward the development of the knowledge needed for the design of new catalysts with good selectivity. This paper is part of a more extensive investigation ongoing in our laboratory into the chemistry of C₃-derived surface moieties adsorbed on transition metal surfaces.^{1–10} C₃ species display a rich thermal chemistry because of the many possible hydrogenation–dehydrogenation reaction pathways available to them, and also because of their potential for skeletal isomerization, metallacycle formation, and carbon–carbon bond coupling reactions.

The thermal decomposition of haloalkanes adsorbed on single-crystal surfaces has become a well-developed method for creating specific hydrocarbon moieties for the purpose of carrying out fundamental studies on their surface chemistry.^{11,12} In this work, the facile thermal cleavage of the C–I and C–Br bonds in allyl iodide and allyl bromide, respectively, results in the deposition of allylic moieties on the surface. This surface species has been previously studied on a few transition metal surfaces, as summarized below.

A high-resolution electron energy loss (HREELS) investigation of the thermal activation of allyl chloride on Ag(110) identified the formation of a π (or η^3) allylic species by 180 K.¹³ Further thermal excitation of this system to 300 K results

in the formation of 1,5-hexadiene, as seen by both HREELS and temperature-programmed desorption (TPD), indicating that silver surfaces favor C–C coupling steps. On Cu(100), the mild thermal activation of allyl bromide also produces 1,5-hexadiene (in this case at temperatures as low as 110 K), but some of the η^3 allyl moieties identified by reflection–absorption infrared spectroscopy (RAIRS) decompose to other surface species.¹⁴ On Ni(100), the dominant desorption products in TPD experiments with allyl chloride are propene and hydrogen,⁷ and the same is true for allyl bromide activation on Al(100)¹⁵ and Pt(111).¹⁶ Coadsorption experiments with deuterium in the latter two studies indicated the production of *d*₂-substituted propene, a result that led the authors to suggest the formation of a C₃ metallacycle intermediate which then undergoes reversible β -hydride elimination followed by incorporation of two deuterium atoms to yield the olefin.

In the work presented here, both allyl iodide and allyl bromide were used to deposit C₃ allylic species on a Pt(111) surface. It will be shown that on clean Pt(111) the molecularly adsorbed allyl halides adopt a gauche conformation with the C–C–C plane close to parallel to the surface, but that in the presence of coadsorbed hydrogen they tilt back toward a more vertical C–C–C plane, a change that facilitates the formation of both cis and gauche isomers. It will also be shown that the decomposition of some surface allyl is essential for its self-hydrogenation to propene and propane, and that allyl hydrogenation can be induced at 100 K lower temperatures when excess hydrogen is preadsorbed on the surface. New insights into the dynamics of the hydrogenation–dehydrogenation steps that can take place on the allyl moieties were obtained by investigating H–D exchange reactions during coadsorption

* Corresponding author.

experiments with allyl iodide and deuterium. The two different hydrogenation processes observed for the allyl precursors can be accounted for by two different adsorption configurations of that intermediate. On one hand, η^1 -allyl hydrogenation results in propene desorption after incorporation of only one deuterium atom. η^3 -allyl hydrogenation, by contrast, produces a di- σ bonded propene intermediate that then undergoes extensive H–D exchange via a cyclic propene–propyl–propene mechanism. Only the η^1 allyl species was directly identified by spectroscopic (RAIRS) means, but our other findings are supported by recent investigations into the thermal chemistry of propene adsorbed on Pt(111).^{1,2} The overall chemistry proposed here for allyl halides on Pt(111) is depicted schematically in Figure 10.

Experimental Section

All temperature-programmed desorption (TPD) data were recorded in an ultrahigh vacuum (UHV) chamber evacuated with a turbomolecular pump to a base pressure in the 6×10^{-11} Torr regime. This chamber is equipped with a quadrupole mass spectrometer retrofitted with an extendible nose cone ended in a 5-mm diameter aperture and placed within 1 mm of the front face of the single crystal for the selective detection of molecules desorbing from that surface. The mass quadrupole is interfaced to a personal computer capable of monitoring the time evolution of up to 15 different masses in a single TPD experiment. The TPD data were recorded using a heating rate of 5 K/s, and are reported in arbitrary units but with relative scales for comparison. A bias of -100 V was placed on the crystal during all TPD experiments to avoid any chemistry induced by the ionizer electrons of the mass spectrometer.² This UHV system also contains a 100-mm concentric hemispherical analyzer and a twin-anode X-ray gun for XPS, a rasterable sputter ion gun for ISS and sample cleaning, and four-grid spherical retarding field optics for LEED. The details of this experimental setup have been published elsewhere.^{17,18}

The reflection–absorption infrared spectroscopy (RAIRS) experiments were performed in a second UHV chamber cryopumped to a base pressure of 5×10^{-11} Torr and equipped with a computer-controlled UTI mass spectrometer for multi-mass TPD and a Bruker Equinox 55 FTIR spectrometer. The infrared beam is focused through a NaCl window onto the platinum crystal at a grazing ($\sim 85^\circ$) incidence, and the reflected light is passed through a polarizer prior to refocusing it onto a narrow band mercury–cadmium telluride (MCT) detector.¹⁹ The entire beam path is purged with a Balston 75-60 air scrubber for CO₂ and water removal. All sample spectra were taken at 4 cm⁻¹ resolution by averaging over 1000 scans, which takes four minutes per experiment, and were ratioed against spectra of the clean sample acquired immediately before. The sample integrity and beam alignment were routinely checked by comparing infrared spectra for a saturation coverage of CO with those reported in the literature.^{20,21}

The platinum single crystal was cut in the (111) orientation and polished to a mirror finish using standard procedures, and mounted via two bridging tantalum wires to a sample holder which could be cooled with liquid nitrogen and/or heated resistively to provide a sample temperature range between 90 and 1200 K, as monitored by a chromel–alumel thermocouple spot-welded to the edge of the crystal. The sample was cleaned between experiments by annealing at 700 K in 3×10^{-7} Torr O₂ to remove any residual carbon, and was periodically monitored for contamination by examining the quality of oxygen TPD.²² Ar⁺ ion sputtering was used sparingly to avoid the creation of surface defects.

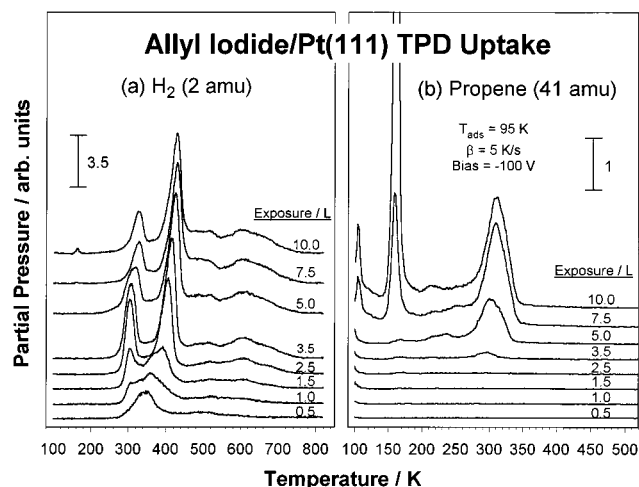


Figure 1. 2 (H₂, left-a) and 41 (propene, right-b) temperature-programmed desorption (TPD) traces from allyl iodide adsorbed on clean Pt(111) as a function of exposure. All dosings were done below 95 K. The metal surface was biased with -100 V in order to avoid damage of the adsorbates by stray electrons from the mass spectrometer ionizer or the ion gauge, and a heating rate of 5 K/s was used in all cases.

Both allyl iodide (98% purity) and allyl bromide (99% purity) were obtained from Aldrich and purified by a series of freeze–pump–thaw cycles, and their purity was checked daily with the mass spectrometer in the chamber. Oxygen (>99.9% purity), CO (>99.9% purity), D₂ (>99.5% atom purity), and propylene (>99% purity) were purchased from Matheson, and used without further purification. Hydrogen (>99.995% purity) was acquired from Liquid Air Products. All exposures are listed in Langmuir (1 L = 1×10^{-6} Torr s), not corrected for ion gauge sensitivities.

Results

3.1. Allyl Iodide Thermal Chemistry on Pt(111). The thermal chemistry of C₃ allyl groups on Pt(111) was first investigated by performing TPD spectroscopy experiments with allyl iodide. Thermal activation of adsorbed allyl iodide on the platinum surface leads mainly to hydrogen and propene desorption along with the production of small amounts of propane. Molecular desorption of the parent allyl iodide was only observed for coverages approaching saturation, demonstrating the facile nature of the C–I bond-scission step. Thermal desorption products resulting from surface-catalyzed C–C coupling reactions were not detected, nor were any stable C₁ or C₂ molecules.

The H₂ (2 amu) TPD data obtained as a function of allyl iodide exposure at 95 K are shown in Figure 1a. At low coverages, hydrogen desorption takes place in a broad temperature range around 350 K, with a small high-temperature tail extending past 700 K. By 1.5 L, however, clear features begin to develop at 305, 360, and 400 K. The peak at 305 K grows quickly and saturates by 3.5 L, but broadens to higher desorption temperatures at 5.0 L, and shifts to 340 K and becomes reduced to nearly half the intensity of its saturated state by 7.5 L. The onset of the development of defined H₂ TPD peaks (3.5 L) coincides with the onset of propene desorption, an observation noted previously in the TPD of allyl bromide on Pt(111).¹⁶ The yield of the 360 K H₂ TPD feature maximizes by 1.5 L, and diminishes afterward.

The hydrogen desorption process seen here between 390 and 460 K is common to TPD spectra from many hydrocarbon

systems, and has been associated, at least in part, with the dehydrogenation of alkylidyne surface species.^{2,23} When a clean Pt(111) surface is exposed to propene this peak is centered at 430 K,² but for the allyl iodide/Pt(111) system the corresponding feature appears around 390 K at low coverages, shifts to 405 K upon saturation at 3.5 L, and continues to shift to higher temperatures until reaching 430 K by 10 L (Figure 1). Both propene and allyl iodide decompose to the same propylidyne species on Pt(111) (see later), so the difference in the behavior of the H₂ TPD peak between the two systems may be due to the presence of iodide or other alkyl intermediates on the surface in the latter case. It is worth noting that a similar shift in this high-temperature hydrogen peak as a function of coverage is also seen in the TPD of 1,3-diiodopropane.⁴ Finally, the broad high-temperature desorption features at 480, 520, 570, 600, and 670 K observed in the H₂ TPD spectra from high coverages of allyl iodide are associated with the stepwise dehydrogenation of the stable surface hydrocarbon fragments that form from the decomposition of propylidyne, ultimately leading to the deposition of surface carbon (by about 800 K).

The dissociation of allyl iodide on Pt(111) at low temperatures produces a surface allyl moiety capable of self-hydrogenation to propene. The TPD spectra of propene (41 amu) from Pt(111) exposed to allyl iodide are presented in Figure 1b. The main peak in these TPD data appears at about 300 K but only after a 3.5 L exposure, and develops with increasing dose, shifting to about 310 K for a 10 L exposure. This behavior compares well with that of propene adsorbed on clean Pt(111), where molecular desorption takes place at approximately 280 K for low coverages and shifts to 270 K upon saturation.² Notice that while the propene desorption profiles are similar in both systems, the associated desorption temperatures do not show similar behavior.

After high exposures to allyl iodide, the 41 amu TPD also displays a peak at 160 K. Comparison of the mass-spectrometer cracking patterns in the TPD data with those of potential products confirms the assignment of this peak to the desorption of molecular allyl iodide. On the other hand, the poorly defined features seen between 200 and 260 K show cracking patterns consistent with desorption of propene, together with small amounts of propane.

Because of the insignificant contribution of propene fragments to the 29 amu signal, propane desorption was primarily monitored with that mass, but the 43 and 44 amu TPD traces were followed simultaneously to support our assignments. The 29 amu TPD data set as a function of Pt(111) exposures to allyl iodide indicates that a small amount of propane desorbs at 305 K starting after a 2.5 L exposure of allyl iodide, the yield increasing with increasing exposure up to a 7.5 L dose (data not shown). Another feature develops at 245 K, but only after 5.0 L of allyl iodide, and that saturates by 10 L. A third small propane feature is observed at approximately 480 K for low exposures to allyl iodide, shifting to 420 K for higher exposures. This latter peak, which reaches a maximum in intensity for the 3.5 L exposure, is also seen in the TPD of propene adsorbed on clean Pt(111), and has been associated with the hydrogenation of propylidyne.²

3.2. Hydrogenation of Surface Allyl Moieties on Pt(111).

When the Pt(111) surface is treated with hydrogen before dosing with allyl iodide, propane desorption begins at lower temperatures, at least 40 K lower than in its absence, and the yield of that alkane increases substantially. The increase in propane production is accompanied by a marked decrease in the propene yield at 310 K, but a new and sharp propene desorption feature

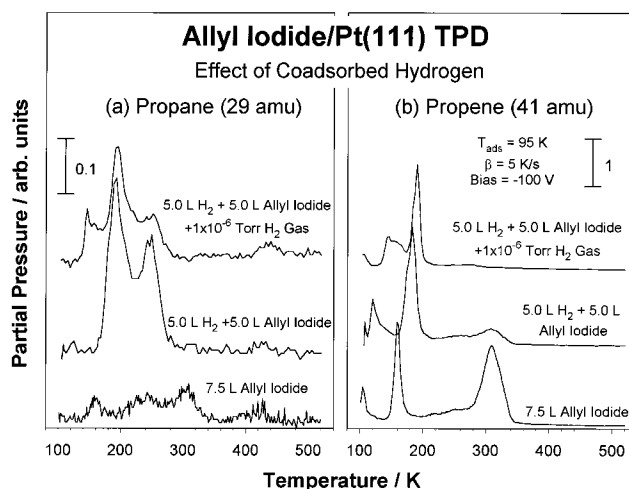


Figure 2. 29 (propane, left-a) and 41 (propene, right-b) amu TPD traces from a study of the influence of coadsorbed hydrogen on the surface chemistry of allyl iodide on Pt(111). The bottom traces correspond to the 7.5 L allyl iodide dose on the clean surface reported in Figure 1. The middle data originate from surfaces predosed with 5.0 L of H₂ prior to allyl iodide adsorption (5.0 L). The surfaces for the top spectra were also prepared by sequentially dosing 5.0 L of H₂ and 5.0 L of allyl iodide, but the TPD experiments in that case were carried out while maintaining a background H₂ pressure of 1×10^{-6} Torr. All adsorptions were done at 95 K.

develops at 185 K. All this suggests that hydrogenation of the surface intermediates in the allyl/Pt(111) system is limited by the availability of surface hydrogen atoms.

The TPD spectra in Figure 2 illustrate this point. The bottom trace in each panel of that figure corresponds to exposures of clean Pt(111) to 7.5 L of allyl iodide, and displays the features described in the previous section. The middle spectrum of Figure 2a shows the propane TPD trace obtained from a surface dosed sequentially with 5.0 L of hydrogen and 5.0 L of allyl iodide. This spectrum shows intense features at 200 and 250 K, indicating that there are two different desorption regimes for propane. The middle spectrum of Figure 2b, which displays the corresponding spectra for propene (41 amu), shows a new sharp peak at 185 K not seen in the case of the adsorption of pure allyl iodide on clean Pt(111). The onset temperature for these hydrogenated desorption products is approximately 160 K.

The upper spectra in Figure 2 were obtained by dosing the Pt(111) surface sequentially with 5.0 L of H₂ and 5.0 L of allyl iodide, as before, but then performing the TPD experiments in the presence of 1×10^{-6} Torr of background H₂. The overall propene and propane yields are lower in this experiment, most likely because of the displacement of some of the iodide by the incoming hydrogen. Nevertheless, the propane (29 amu) peak at 200 K does grow relative to that at 250 K, further highlighting the fact that the availability of surface hydrogen lowers the desorption temperature of propane. In the presence of 1×10^{-6} Torr H₂, the propene peak at 305 K shrinks to the limits of detection, and the 185 K peak shifts to 195 K. The additional feature that grows in the 29 and 41 amu TPD traces at about 150 K with a broad shoulder toward its high-temperature side has a cracking pattern consistent with that of molecular allyl iodide.

3.3. Desorption Yields. To gain a better insight into the thermally activated mechanism for allyl iodide conversion on Pt(111), the desorption yields in the TPD data presented above were quantified. The areas under the individual hydrogen TPD peaks were calibrated against those from H₂-dosed Pt(111), and converted into absolute coverages by using the fact that an

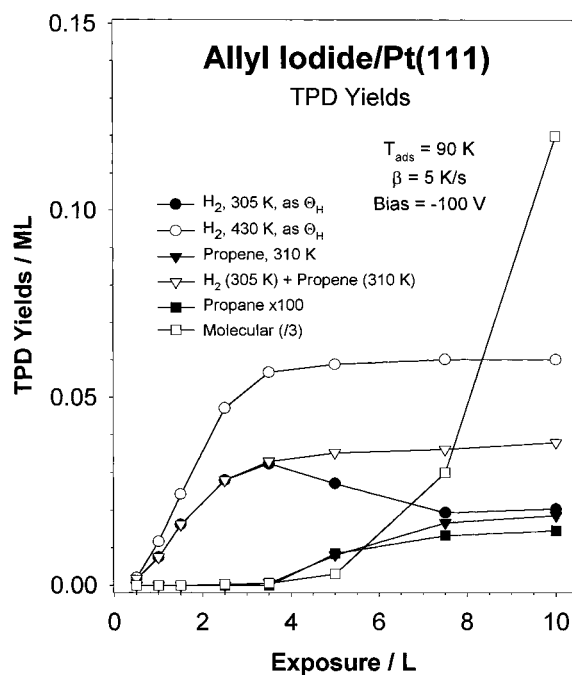


Figure 3. TPD yields as a function of exposure for allyl iodide adsorbed on clean Pt(111), as calculated from the data in Figure 1 after appropriate calibration. Reported here are the yields for the 305 and 430 K H_2 TPD peaks (as Θ_H), for the main 310 K propene feature, for propane, and for molecular allyl iodide. Also displayed is the evolution of the combined yield of propene and the 305 K H_2 peak to highlight the interdependence of those two features.

exposure of 30 L of hydrogen results in the buildup of 0.6 monolayers of atomic hydrogen (1 ML = 1:1 ratio of adsorbate to substrate surface atom).²⁴ The yields for propene and propane desorption were then estimated by comparing the mass spectrometer relative sensitivities to those compounds with respect to hydrogen. Provided in Figure 3 are plots for the 305 and 430 K H_2 , the 310 K propene, the total propane, and the parent allyl iodide desorption yields as a function of Pt(111) exposure to allyl iodide. The figure also shows the evolution of the sum of the yields of hydrogen at 305 K and propene at 310 K after proper scaling.

The yields of both 305 and 430 K hydrogen desorption processes increase almost linearly with allyl iodide doses up to 2.5 L, at which point the 430 K H_2 desorption yield levels off to a constant value at about 0.06 ML. The yield for the 305 K H_2 desorption process displays a similar behavior to the 430 K process up to 3.5 L, but then goes down at higher exposures. This reduction in yield is accompanied by the onset of propene desorption, as already mentioned, presumably because the surface allyl species requires an extra hydrogen to hydrogenate to propene and this extra hydrogen is supplied by the decomposition of some of the allyl surface species. The maximum amount of propene that desorbs from surface allyl hydrogenation on the clean surface is 0.018 ML.

The total amount of propane detected in the TPD experiments after allyl iodide saturation was 0.00015 ML. However, when the Pt(111) surface is treated with 5.0 L H_2 prior to the 5.0 L exposure to allyl iodide, more than 0.01 ML propane is produced. In that case, the propene peak at 305 K is reduced to 1/3 of its original intensity, but that is more than compensated by the development of a new propene feature at 185 K, so the total propene desorption yield in the presence of hydrogen reaches 0.025 ML, higher than the 0.018 ML produced in the absence of preadsorbed hydrogen.

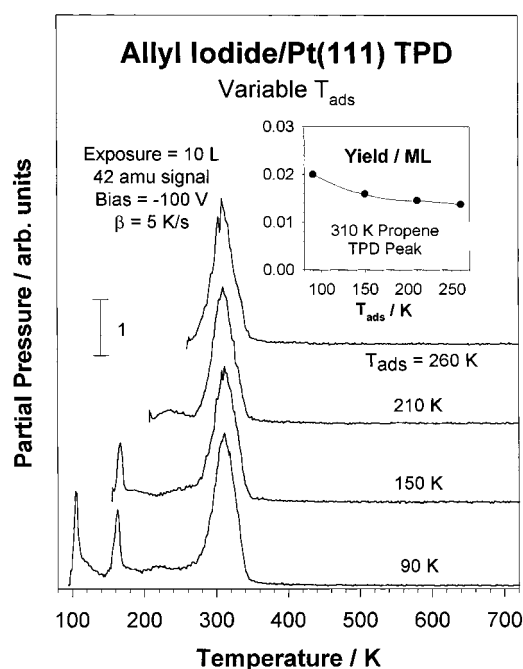


Figure 4. 42 (propene) amu TPD data for 10 L of allyl iodide adsorbed on clean Pt(111) as a function of dosing temperature. Four cases are shown here, for $T_{ads} = 90, 150, 210,$ and 260 K. The yields of the 310 K propene TPD peak as a function of T_{ads} is displayed in the inset.

3.4. Allyl Iodide Adsorption as a Function of Temperature.

TPD experiments were also performed as a function of allyl iodide adsorption temperature for two exposure regimes: 5.0 L, where no molecular desorption occurs, and 10 L, where allyl iodide desorbs intact for adsorption temperatures below 160 K. The 42 amu TPD traces recorded from the latter set are shown in Figure 4. In both exposure regimes, the propene yields at 310 K are approximately constant up to adsorption temperatures of 260 K (an overall reduction in propene yield of about 20% is seen when adsorbing at 260 K, see inset), and the yields of the other relevant desorbing species remain in constant proportion to each other throughout the range of adsorption temperatures (data not shown). These results do not conform with previous work with allyl bromide,¹⁶ for which a 5-fold increase in propene yield was reported as the adsorption temperature decreases from 300 to 100 K, but this discrepancy could be related to the different exposures used in both experiments. Our data imply that the precursor to allyl hydrogenation is formed at low temperatures, and that such precursor is stable on the surface until the hydrogen needed for the hydrogenation steps becomes available.

3.5. H–D Exchange. When allyl iodide is thermally activated in the presence of coadsorbed deuterium, a wide distribution of isotopomers desorb from the surface because of the extensive H–D exchange that takes place on the surface. Indeed, the TPD results recorded after sequentially dosing 5.0 L of deuterium and 5.0 L of allyl iodide presented in Figure 5 show the desorption of numerous deuterated ion fragments.

The left panel of Figure 5 shows the TPD traces for 2 (H_2), 3 (HD), and 4 (D_2) amu. In these, it is seen that most of the deuterium desorbs in the form of D_2 , and that it does so by 300 K. Nevertheless, a substantial amount of deuterium does desorb as HD in a sequence of steps between 150 and 800 K. Note in particular that any HD desorbing above 350 K must originate from processes involving deuterium atoms incorporated into hydrocarbon surface fragments, with rates limited by the surface reactions that release that deuterium. For example, the sharp

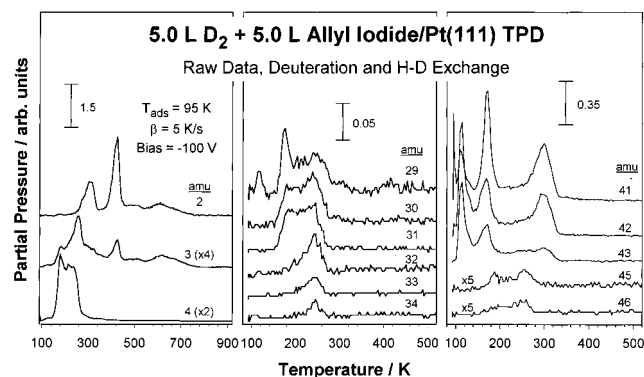


Figure 5. 2 (H₂), 3 (HD), and 4 (D₂, left), 29–34 (C₂H₃D_{3–x}⁺, center), and 41–46 (C₃ fragments, right) amu TPD traces for the case of a 5.0 L allyl iodide dose on Pt(111) previously exposed to 5.0 L of D₂. Monodeuterated propene desorption is identified at 170 and 300 K by peaks in the 29, 41, 42, and 43 amu traces, and multiply exchanged propane is detected around 250 K in all 29–34 and 41–46 amu data.

desorption peak at 430 K in the 3 amu (HD) TPD trace shows that the decomposition of propylidyne involves deuterium. This is a clear indication that extensive deuterium incorporation into the surface hydrocarbon species takes place at low temperatures.

The D₂ + allyl iodide 29–34 amu TPD profiles are shown in the center panel of Figure 5. These masses are identified mainly with the possible C₂⁺ fragments that form during propene and propane decomposition in the ionizing region of the mass spectrometer. Some interesting observations from this data set are quite informative about the reaction mechanism involved in the H–D exchange processes. First, let us consider the 29 amu desorption trace, which corresponds to either the C₂H₅⁺ fragment of normal propane or the C₂H₃D⁺ fragment of deuterated propenes. The first peak in that trace at 170 K is coincident with the propene desorption peaks in the 41, 42, and 43 amu data (right-hand panel), and it is therefore assigned to the desorption of CH₂=CHCH₂D. Notice that this peak is not present in the 30–34, or ≥44 amu TPD traces, and that its desorption maximum is at least 20 K lower than that of propane. The desorption of monodeuterated propene in this temperature range implies that the surface allyl species must hydrogenate via the direct incorporation of one single hydrogen (deuterium) atom under those conditions. The propene peak at 300 K exhibits some common characteristics to the peak at 170 K, in that it only shows intensity in the TPD traces up to 43 amu (no H–D exchange takes place in that desorption regime either).

Next, the 30 (C₂H₄D⁺) and 31 (C₂H₃D₂⁺) amu TPD traces display a peak at about 190 K not visible in the data for 32 (C₂H₂D₃⁺) amu. This argues for the direct deuteration of CH₂=CHCH₂D to propane-*d*₃, the CH₂DCHDCH₂D isotopomer, without the occurrence of any further H–D exchange. Additional evidence for this mechanism is provided in Figure 6, which shows the allyl iodide/Pt(111) 43–48 amu TPD desorption traces for two different co-exposures of deuterium. The dominant contributions to those masses is from the appropriate propane isotopomers (C₃H₈ for 44 amu to C₃H₄D₄ for 48 amu). In both deuterium exposure regimes, significant intensity is seen at 190 K only up to 47 amu, which represents the C₃H₅D₃ isotopomer. Finally, returning to the center panel of Figure 5, the intensities seen at 250 K for all mass from 29 to 34 (together with the appropriate signals in the 43–48 amu traces in Figure 6) indicate the desorption of all possible isotopomers of propane, which implies extensive H–D exchange in that case.

To check further on the chemistry of allyl groups discussed above, a few TPD spectra were also recorded for Pt(111)

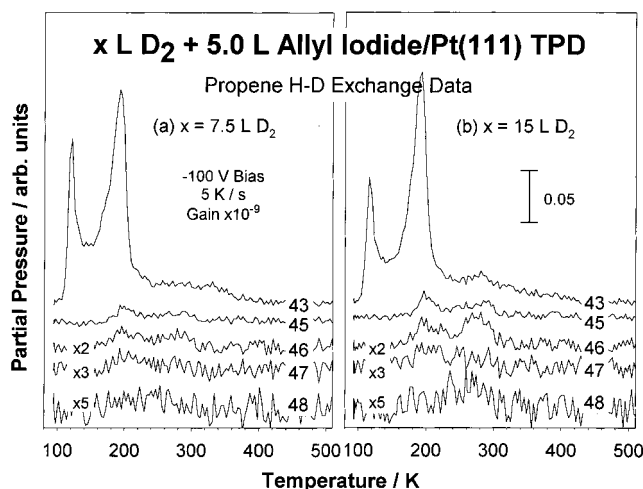


Figure 6. 43, 45, 46, 47, and 48 amu TPD traces for 5.0 L of allyl iodide adsorbed on Pt(111) predosed with either 7.5 (left) or 10 (right) L of D₂. These data reinforce the detection of multiply H–D exchanged propane also identified by the spectra in Figure 5.

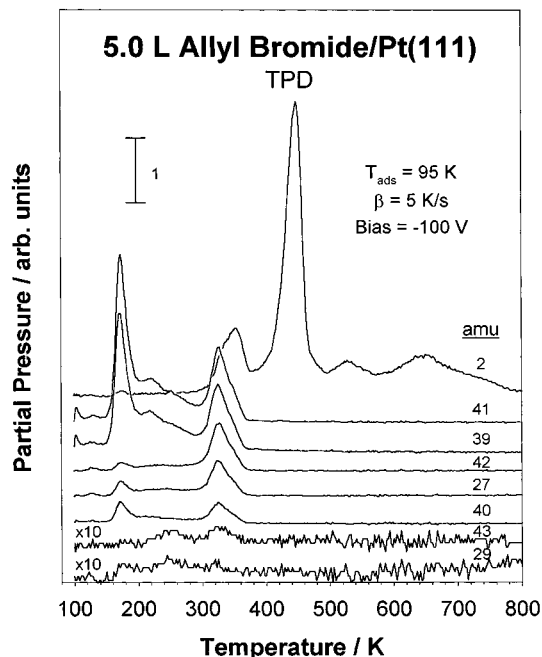


Figure 7. 2 (H₂), 41, 39, 42, 27, and 40 (propene), and 43 and 29 (propane) amu TPD traces for 5.0 L of allyl bromide adsorbed on clean Pt(111). These results match quite closely those obtained with allyl iodide, illustrating the similar chemistry in both cases because of the initial formation of the same surface allylic intermediates.

exposed to allyl bromide. Figure 7 shows the 2 (H₂), 27, 39, 40, 41, and 42 (propene), and 29 and 43 (propane) amu TPD traces recorded for the case of 5.0 L of allyl bromide. Some subtle differences are seen between these data and those from allyl iodide, among them the relative higher intensities of the 340 and 440 K hydrogen desorption peaks in the former, which are likely to be due to a coverage effect (since bromine atoms are smaller than iodine atoms). Also, the broad feature at about 230 K in the 41 amu TPD is larger in the case of allyl bromide, even though mass spectrometer cracking patterns indicate that there is some contribution from molecular desorption at this temperature range. These are minor differences, however; the important thing to realize is that the thermal chemistry of both systems is essentially the same.

3.6. RAIRS. RAIRS was used to spectroscopically identify the surface adsorbates that form by thermal activation of allyl

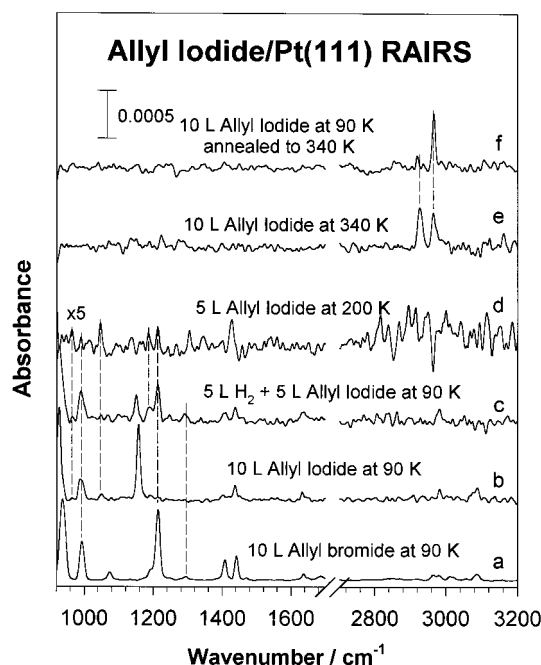


Figure 8. Reflection-absorption infrared spectra (RAIRS) used to identify the key surface intermediates involved in the chemistry of allyl halides on Pt(111). From bottom to top, these data correspond to: (a) 10 L of allyl bromide adsorbed molecularly on the clean platinum at 90 K; (b) 10 L of molecular allyl iodide adsorbed on clean Pt(111) at 90 K; (c) 5.0 L of molecular allyl iodide dosed at 90 K on a 5.0 L H_2 -predosed Pt(111); (d) 5.0 L of allyl iodide adsorbed on clean Pt(111) at 200 K (at which point the C–I bond dissociates to yield a surface η^1 allylic species); (e) 10 L of allyl iodide adsorbed on clean Pt(111) at 340 K; and (f) 10 L of allyl iodide adsorbed on clean Pt(111) at 90 K and annealed to 340 K. The latter two traces correspond to surface propylidyne.

halides on Pt(111). Three temperature regimes were investigated: 90 K, where molecular adsorption is expected; 200 K, where, according to the TPD data, the formation of a surface allylic moiety is likely; and 340 K, at which point propylidyne forms on the surface. Shown at the bottom of Figure 8 are RAIRS of Pt(111) exposed to 10 L of allyl bromide (a), 10 L of allyl iodide (b), and 5.0 L of allyl iodide coadsorbed with 5.0 L of hydrogen (c), all at 90 K. The mode assignment for these data was done by comparison with the infrared spectra of the respective allyl halides in the liquid and vapor phases found in the literature,²⁵ and is reported in Table 1. The relative intensities of the different peaks in these RAIRS data can be used to infer the adsorption geometries of the halides. A more detailed description of this is provided in the discussion.

In terms of the identification of the surface intermediates formed after the dissociation of the carbon–halogen bonds, Figure 8d displays the RAIRS trace recorded from Pt(111) exposed to 5.0 L of allyl iodide at 200 K. The RAIRS signals in that spectrum are rather weak, but some peaks are nevertheless distinguishable above the noise at 963, 990, 1046, 1185, 1212, 1304, and 1427 cm^{-1} ; those features were consistently reproduced in experiments carried out on different days. Assignments of the vibrational modes for this spectrum are also presented in Table 1, and discussed in the next section.

Finally, the surface intermediate that forms by adsorption of allyl iodide on Pt(111) above 300 K was clearly identified as propylidyne. The formation of this intermediate was achieved both by exposure of Pt(111) to allyl iodide directly at 340 K (Figure 8e), and by exposure of Pt(111) to allyl iodide at 90 K followed by annealing to 340 K (Figure 8f). In both instances, the RAIRS peaks at 2925 and 2965 cm^{-1} associated with a

propylidyne species¹ were clearly observed. There are, however, some differences in the relative intensities of those peaks depending upon the method of preparation used, indicating subtle changes in adsorption geometries between the two cases (see below). By comparing with the data from the propene/Pt(111) system,¹ the intensities of those peaks are estimated to correspond to propylidyne coverages slightly above 0.10 ML, a bit more than those seen with propyl iodide.³ This estimate is also somewhat higher than the ~ 0.03 ML obtained from TPD (Figure 4).

Discussion

4.1. Allyl Halide Molecular Adsorption on Pt(111). As mentioned above, the adsorption geometries of allyl iodide and allyl bromide were investigated by RAIRS. Based on the surface dipole selection rule in RAIRS, which establishes that only vibrational modes with dynamic dipoles that have a perpendicular component can be seen on metal surfaces,^{26–28} the adsorption geometries for allyl iodide and allyl bromide on the clean Pt(111) surface could be determined. In the following section we discuss how these assignments were made.

The bending modes of the methylene group ($-CH_2X$) are examined first. The methylene twisting modes seen in the liquid phase as weak absorptions at 1071 cm^{-1} for allyl bromide and 1050 cm^{-1} for allyl iodide are also visible in the spectra for the surface-bonded species, at 1073 and 1050 cm^{-1} , respectively. The twisting dynamic dipole is perpendicular to the plane of the CH_2 group, so the most likely adsorption configuration that would accommodate this observation is an end-on bonded allyl halide via the halogen atom and with the carbon–halogen bond approximately perpendicular to the surface. In addition, the methylene scissoring mode at 1440 cm^{-1} for allyl bromide is stronger (in relative terms) than the equivalent mode at 1436 cm^{-1} for allyl iodide. Such difference could be accounted for by tilting of the C–Br bond toward the plane of the surface, a change that would increase the perpendicular dipole component of this mode in RAIRS, and would result in a stronger peak in the bromide case. Finally, the methylene wagging modes, at 1212 cm^{-1} for allyl bromide and 1156 cm^{-1} for allyl iodide, correspond exclusively to the allyl halide gauche isomer, and are quite strong in the spectra of the adsorbed species. No modes assignable to the cis isomer are seen on the clean Pt(111) surface, but when allyl iodide is coadsorbed with hydrogen, signals for both the cis and gauche isomers appear at 1212 and 1150 cm^{-1} , respectively.²⁹ This means that the vinyl group of the adsorbed molecule must adopt two orientations in that case, one pointing toward the surface, and another away from it.

Additional information can be extracted from the vibrational modes of the end $=CH_2$ vinyl group. In particular, the vinyl twisting mode at 1192 cm^{-1} for allyl bromide appears to be stronger than the equivalent mode for allyl iodide (whereas in the gas phase this mode displays similar intensities for both allyl halides). Again, provided that the molecules adopt a gauche configuration with the C–C–C plane close to parallel to the surface, the proposed tilting of the C–Br toward the surface plane is consistent with the increased visibility of this mode, and conversely, a more upright geometry in allyl iodide justifies the weaker absorbance in that case. Also, there is a slight strengthening of the in-plane vinyl CH_2 bend (scissoring) mode at 1409 cm^{-1} for allyl iodide coadsorbed with hydrogen (compared to neat allyl iodide), which can be interpreted as a tilting back of the C–I bond so that that vinyl CH_2 group is lifted away from the surface.

The vinyl middle C–H vibrational modes complement the previous assignments. First, the out-of-plane vinyl hydrogen

TABLE 1: Assignment of the Vibrational Frequencies Seen in the Infrared Spectra of Allyl Bromide and Allyl Iodide in Their Pure Liquid States²⁵ and Adsorbed on Pt(111) (all frequencies are reported in cm⁻¹)

assignment ^{a,b}	liquid allyl bromide		liquid allyl iodide		10 L allyl bromide on Pt(111), 90 K	10 L allyl iodide on Pt(111), 90 K	5 L H ₂ + 5 L allyl iodide on Pt(111), 90 K	5 L allyl iodide on Pt(111), 200 K
	gauche	cis	gauche	cis				
$\nu(\text{C}=\text{C})$	1638 s	1647 m	1632 s	1645 m	1636 w	1631 m	1637 w	
$\gamma(\text{CH}_2)_{\text{methylene}}$	1442 m		1439 m		1440 m	1436 m	1436 w	
$\gamma(\text{CH}_2)_{\text{vinyl}}$	1409 m		1405 m	1420 w	1407 m	1401 w	1409 w	1427 m
$\delta_{\text{ip}}(\text{CH})$	1294 w		1292 w		1293 w		1290 w	1304 w
$\omega(\text{CH}_2)_{\text{methylene}}$	1208 s	1245 w	1150 s	1201 w	1212 s	1156 s	1212, 1150 s	1212 w
$\tau(\text{CH}_2)_{\text{vinyl}}$	1195 w	1042 w	1187 w	1022 w	1192 sh		1188 m	1185 w
$\tau(\text{CH}_2)_{\text{methylene}}$	1071 w	1154 w	1050 w	1088 w	1073 w	1050 w	1047 w	1046 m
$\delta_{\text{oop}}(\text{CH})$	984 s		981 s		992 s	988 m	990 s	990 w
$\nu_{\text{ip}}(\text{C}-\text{C})$	935 sh		932 sh			964 w	964 w	963 w
$\delta_{\text{oop}}(\text{CH})$	926 s		928 s		933 s	927 s	927 s	

^a Modes: ν = stretching, γ = scissoring, δ = deformation, ω = wagging, τ = twisting, ip = in-plane, oop = out-of-plane. ^b Intensities: s = strong, m = medium, w = weak, sh = shoulder.

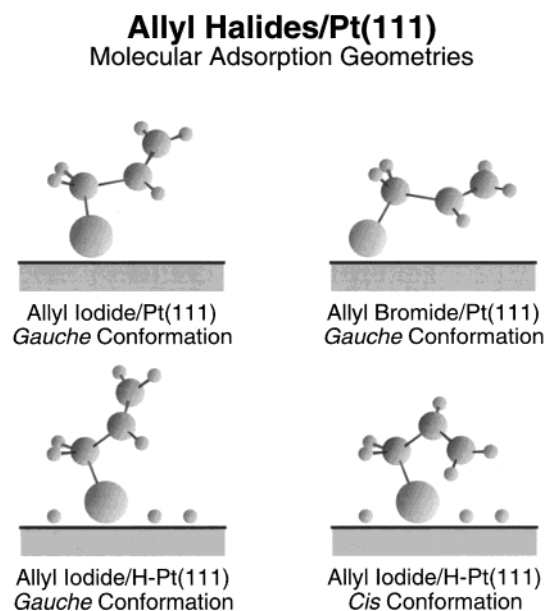


Figure 9. Proposed adsorption geometries for allyl bromide and allyl iodide on clean and hydrogen-predosed Pt(111). These were inferred from RAIRS data, and correspond to the molecular adsorbates obtained near saturation coverages.

bend for allyl bromide (992 cm⁻¹) is stronger in relative terms than the equivalent mode for allyl iodide (988 cm⁻¹), suggesting a lateral tilt of the vinyl C–H bond toward the plane of the surface in the former case. Second, the tilting of the C–I bond upon hydrogen coadsorption is also expected to orient the vinyl C–H bond toward the plane of the surface, and as such to make the vinyl C–H in-plane bend mode more visible in RAIRS, and this is what is observed: a relatively strong vinyl C–H in-plane bend is seen there at 1188 cm⁻¹. Last, the tilting back reduces the hindrance expected for the vinyl CH₂ group of the cis isomer with the surface.

The last peak to be assigned is that seen at about 964 cm⁻¹ in the case of allyl iodide, which has been previously associated with a C–C–C in-plane stretching mode.^{13,25,30} The observation of this peak in our spectra again points to a geometry with the molecular plane tilted away from the surface plane. This is also supported by the observation of the C=C stretch at about 1631 cm⁻¹ on clean Pt(111) and at 1637 cm⁻¹ when hydrogen is predosed. A schematic of the proposed geometries is shown in Figure 9.

4.2. Surface Allyl Formation. Exposure of Pt(111) to allyl iodide at 200 K is believed to result in a dissociative adsorption, in which the C–I bond cleaves and yields a surface-bonded

allylic moiety. The RAIRS of this intermediate is shown in Figure 8d, and the corresponding peak assignments are made in Table 1. The first thing to notice from these data is that some peaks in the spectrum of the 200 K surface intermediate match quite closely those from the molecular species, and that others are at least in the same vibrational regions. These similarities strongly suggest that the species that forms after adsorbing allyl iodide on Pt(111) at 200 K is a η^1 allylic moiety. Conversely, little correspondence can be found between the surface vibrational spectrum of the allyl moiety at 200 K and those from organometallic π allyl complexes.^{30,31} We therefore identify the species formed by thermal activation of allyl halides to one with a η^1 allylic structure, at least at high coverages. A relative increase in the signals of the C–C stretching at 963 cm⁻¹, the methylene CH₂ twisting at 1046 cm⁻¹, the vinyl C–H in-plane bending at 1304 cm⁻¹, and the vinyl CH₂ in-plane bending (scissoring) at 1427 cm⁻¹, are accompanied by a weakening of the vinyl C–H out-of-plane bending at 990 cm⁻¹. All this points to a η^1 allylic adsorbate with the C–C–C plane tilted up toward a perpendicular configuration.

4.3. Allyl Hydrogenation. The chemistry of C₃ allyl moieties on Pt(111) previously established from TPD studies with allyl bromide¹⁶ was in general terms reproduced here with allyl iodide. In addition, new findings related to the interaction of propene with Pt(111)^{1,2} have enabled us to identify some thermally activated reactivity features in the allyl halide/Pt(111) system not noted previously. Two observations of particular interest from this study are the low-temperature hydrogenation reactions induced by hydrogen pre-dosing, and the H–D exchange reactivity of allyl surface groups in the presence of coadsorbed deuterium.

The hydrogenation reactions seen when allyl iodide is adsorbed on clean Pt(111) will be discussed first. In that case, the onset of the propene desorption process is centered at 310 K, occurs only for exposures in excess of 2.5 L (Figure 1), and is accompanied by a decrease in yield in the 305–340 K hydrogen desorption (Figure 3). The overall yield of the H₂ peak is governed by a competition between hydrogenation and dehydrogenation reactions with the surface allyl species. That the desorbing hydrogen does indeed originate from the decomposition of surface allylic species is evidenced by results from our laboratory with partially deuterated 1,3-diiodopropane.⁴ In brief, the hydrogen TPD spectra of ICD₂CH₂CD₂I display signals at 235 K only for H; no desorbing D is detected at that temperature. This means that the first dehydrogenation process in platinacyclobutane is β -hydride elimination to a surface allylic moiety. The further decomposition of this allylic species is signaled by the onset of deuterium desorption, and this occurs

Allyl Thermal Chemistry on Pt(111)

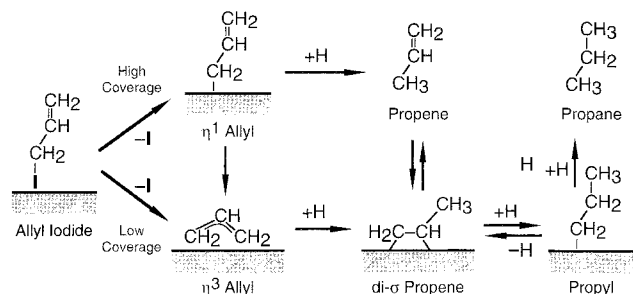


Figure 10. Schematic representation of the reaction mechanism proposed for the thermal chemistry of allylic moieties on Pt(111) surfaces.

at 340 K. In that light, the observed decrease in yield with coverage in the 305–340 K hydrogen desorption peak from allyl iodide seen here must result from hydrogen scavenging by the allyl moiety. The fact that this decrease only occurs at coverages above a critical value can be explained by (1) a blocking of empty sites for dehydrogenation, which also makes hydrogenation of surface allyl moiety more viable; and (2) a geometrical rearrangement of the allyl moiety due to surface crowding which facilitates hydrogenation. The latter idea in particular is quite appealing, and was first proposed by White et al. in their investigation of the chemistry of allyl bromide on Pt(111).¹⁶ They suggested that at some critical coverage, the dissociative adsorption of allyl bromide leads to the formation of allyl species with a η^1 configuration, and that this η^1 allyl moiety reductively eliminates to propene once surface hydrogen from η^3 allyl dehydrogenation becomes available. Our RAIRS data provides direct evidence for the η^1 allylic configuration, and the reduction in H_2 TPD yield with coverage matching the propene produced supports the proposed hydrogenation step.

Further insight into the allyl-to-propene conversion process at 310 K can be obtained by comparison with thermal desorption data from direct adsorption of propene on clean Pt(111). One difference between the two systems is that the desorption of adsorbed propene occurs at approximately 40 K lower temperatures than where the main propene desorption peak is seen for allyl iodide. It is unlikely for this difference to be due to the presence of surface iodine, because other propene and propane desorption features show common behavior in both adsorption systems (see below). Instead, the main (310 K) propene TPD feature from allyl iodide on Pt(111) is likely to be limited by the dehydrogenation of some of the allyl moieties. It is suggested here that, in the absence of H_{ads} , the allyl moieties form on the surface below 160 K but do not dissociate until about 270 K.

When hydrogen is made available on the surface (by predosing H_2), the allyl hydrogenation process at 310 K is substantially suppressed in favor of a low-temperature hydrogenation step around 185 K (Figure 2). This indicates that the C_3 intermediates that hydrogenate to propene must form on the surface below 160 K, the onset temperature for this propene and propane desorption. This idea is also supported by the fact that almost no changes in yields are detected for the hydrogen, propene, or propane that desorb in the TPD experiments with allyl iodide as a function of adsorption temperature. The reaction mechanism for the low-temperature hydrogenation reactions of the surface allyl moiety proposed here is shown schematically in Figure 10.

Finally, additional information on the hydrogenation of allyl moieties at 310 K with surface hydrogen was obtained by TPD experiments with coadsorbed deuterium. In these experiments,

the desorption of all the isotopomers of propene were followed, but desorption intensity was only detected for masses up to 43 amu, that is, for monodeuterated propene (C_3H_5D), the same as in the 185 K peak (Figure 5). This suggests the incorporation of only one deuterium atom into allyl moieties without further H–D exchange.

4.4. Coordination of Surface Species. It is interesting to speculate on the adsorption geometry of the allyl species that hydrogenate to propene. Both the 310 K propene TPD peak from allyl iodide adsorbed alone on clean Pt(111) and the 185 K feature that develops upon hydrogen or deuterium coadsorption incorporate only one H (D) surface atom, and are therefore likely to be bonded in a η^1 configuration. Direct evidence for this intermediate is indeed available from the RAIRS data. On the other hand, some allyl moieties do decompose on the surface (hence the availability of hydrogen at ~ 300 K for propene desorption), and that requires more extensive coordination to the metal. Moreover, some of the propene produced below 200 K remains on the surface, and later decomposes to propylidyne or hydrogenates to propane. This argues for another allyl configuration, perhaps a η^3 intermediate.

On the basis of these considerations, it is possible for both η^1 and η^3 allyl moieties to coexist on the surface. The α -carbon of the η^1 allyl is expected to hydrogenate directly and desorb as propene, whereas when η^3 allyl hydrogenates it forms a di- σ bonded propene intermediate that then either desorbs as propene or hydrogenates further and desorb as propane. This is seen in the extensive H–D exchange reported in Figure 5. We propose that the formation of η^1 and/or η^3 allyl intermediates depend on the coverages of the surface species.

The desorption of multiply H–D exchanged propane and propene from allyl iodide adsorbed on deuterium-predosed Pt(111) warrants further discussion. Let us focus on the center panel of Figure 5, which shows the 29 amu ($C_2H_3D^+$) TPD trace obtained when 5.0 L of D_2 is coadsorbed with 5.0 L of allyl iodide. A sharp peak at 170 K, coincident with the features at 170 K in the 41–43 amu TPD spectra in the right-hand panel of the same figure, is identified with a singly deuterated propene molecule, C_3H_5D . Since that peak does not appear in the 30–34 amu TPD traces, it is concluded that no H–D exchange occurs during the hydrogenation process at that temperature. This observation could be the consequence of one of three possible scenarios: (1) the replacement of the iodine atom in molecularly bonded allyl iodide molecules by a deuterium atom in a concerted displacement step which yields C_3H_5D without the formation of any new surface intermediate; (2) the immediate ejection of propene from the surface once the η^1 allylic intermediate incorporates the extra hydrogen; or (3) the inhibition of the reversible propyl–propene reaction involved in H–D exchange once propene is formed (perhaps because surface crowding). We argue that the latter suggestion is more likely, because deuterated propanes with fragments up to 31 amu ($C_2H_3D_2^+$) also desorb at 180 K. This means that some of the C_3H_5D molecules that form at 170 K are likely to adsorb into a di- σ bonded configuration which then allow for the addition of two deuterium atoms sequentially to form a propyl group first and $CH_2DCHDCH_2D$ afterward (identified by the 31 and 47 amu TPD peaks at 180 K).

Hydrogenation of allyl moieties to a C_3 metallacycle has been suggested previously as an alternative reaction pathway for propane- d_3 production,¹⁶ but our associated study of the chemistry of C_3 metallacycles on Pt(111) has shown that such intermediate is likely to undergo fast β -H elimination back to the allyl, and to hydrogenate via propene and propyl formation.⁴

No evidence was obtained in our work for the possibility of a C₃ metallacycle forming from allylic precursors. On the other hand, previous investigations in our laboratory have shown that the sequential exposure of Pt(111) to deuterium and propene results in the thermal desorption of multiply exchanged propene and propane at 250 K in a process involving the reversible formation of surface propyl groups.² Similar features are seen in the experiments with allyl iodide reported here, namely: (1) the desorption of deuterium-substituted propenes is accompanied by the desorption of deuterium-substituted propanes; (2) all possible deuterium-substituted propane (up to d₈) isotopomers are detected; and (3) unexpectedly low desorption yields for propane-d₁ and propane-d₃ are observed.

4.5. Propylidyne Formation. Finally, we report on the production of propylidyne on Pt(111) via thermal activation of allyl iodide around room temperature. Indeed, the exposure of Pt(111) to 10 L of allyl iodide at 90 K followed by annealing at 340 K produces a RAIRS trace with two clearly visible peaks at 2925 and 2965 cm⁻¹. Those peaks are easily assignable to the symmetric and asymmetric CH₃ stretches, respectively.¹ Furthermore, because of the particularly large intensity of the asymmetric stretch, we propose that the terminal methyl group in this system is oriented with its main axis tilted close to the surface plane. Exposing Pt(111) to allyl iodide directly at 340 K, on the other hand, results in a marked increase in the intensity of the symmetric stretching mode. This can be interpreted as the result of a more upward configuration of the terminal methyl group due to tighter packing of the propylidyne layer. A higher coverage is expected (and seen) in this latter case.

The hydrogen TPD data supports the formation of propylidyne. In particular, the H₂ TPD peak between 390 and 460 K is typical of the conversion of that species to an intermediate of C₃H₂ stoichiometry. On the basis of the discussion presented above, it is proposed that the formation of propylidyne on Pt(111) occurs via the thermal activation of the propene produced by allyl hydrogenation, not by any direct rearrangement of the allyl surface moiety.² Our extensive studies on the chemistry of ethylene on Pt(111) also lead us to propose that hydrogenation of the surface allyl moiety to di-σ propene is followed by a 1,2 hydrogen shift to propylidene (Pt₂=CH-CH₂-CH₃), which then α-hydride eliminates to propylidyne.^{23,32-39}

Conclusions

The adsorption geometries of allyl bromide and allyl iodide on Pt(111) were investigated by using RAIRS. For both adsorbates, end-on bonding through the halogen atom with the C-C-C plane close to parallel to the surface in a *gauche* conformation is proposed. In the presence of coadsorbed hydrogen, an upward tilt of allyl iodide is induced, so the C-C-C plane adopts a more perpendicular configuration; both *cis* and *gauche* isomers were identified in that case. Molecularly adsorbed allyl halides can be thermally activated to produce a C₃ surface allylic species. A η¹ allylic species was identified at 200 K directly by RAIRS, and the formation of an additional η³ intermediate was inferred from the TPD data with coadsorbed hydrogen and deuterium.

In terms of the desorption data, only hydrogen is observed from thermal activation of allyl moieties at low coverages, in two main processes around 305–340 K (representative of surface allyl dehydrogenation), and between 400 and 430 K (associated with propylidyne dehydrogenation). After high allyl iodide exposures, on the other hand, significant amounts of propene are also detected in the gas phase. Deuterium-labeling

experiments show that this alkene is mainly produced by direct hydrogenation of η¹ allylic moieties. The desorption temperatures for propene on clean Pt(111) are higher than expected from experiments with the pure olefin, because hydrogenation cannot take place until hydrogen from allyl decomposition becomes available. In the presence of coadsorbed hydrogen, however, hydrogenation of allyl moieties can be substantially facilitated. Two low-temperature hydrogenation pathways can in fact be triggered by this procedure. The first, occurring between 170 and 210 K, produces propene together with a small amount of propane via a direct hydrogen incorporation mechanism into η¹ allyl that does not involve any H-D exchange. The second process, which takes place between 210 and 280 K, produces relatively more propane, most likely involves an initial η³ allylic species, and includes extensive H-D exchange via a propene-propyl-propene surface interconversion mechanism.

Acknowledgment. Financial support for this project was provided by the National Science Foundation under Grant No. CHE-9819652.

References and Notes

- (1) Zaera, F.; Chrysostomou, D. *Surf. Sci.* **2000**, *457*, 71.
- (2) Zaera, F.; Chrysostomou, D. *Surf. Sci.* **2000**, *457*, 89.
- (3) Chrysostomou, D.; French, C.; Zaera, F. *Catal. Lett.* **2000**, *69*, 117.
- (4) Chrysostomou, D.; Chou, A.; Zaera, F. *J. Am. Chem. Soc.*, submitted.
- (5) Tjandra, S.; Zaera, F. *Langmuir* **1994**, *10*, 2640.
- (6) Tjandra, S.; Zaera, F. *J. Am. Chem. Soc.* **1995**, *117*, 9749.
- (7) Tjandra, S.; Zaera, F. *J. Phys. Chem. B* **1997**, *101*, 1006.
- (8) Jenks, C. J.; Bent, B. E.; Bernstein, N.; Zaera, F. *J. Am. Chem. Soc.* **1993**, *115*, 308.
- (9) Jenks, C. J.; Bent, B. E.; Bernstein, N.; Zaera, F. *J. Phys. Chem. B* **2000**, *104*, 3008.
- (10) Jenks, C. J.; Bent, B. E.; Zaera, F. *J. Phys. Chem. B* **2000**, *104*, 3017.
- (11) Zaera, F. *Acc. Chem. Res.* **1992**, *25*, 260.
- (12) Zaera, F. *Chem. Rev.* **1995**, *95*, 2651.
- (13) Carter, R. N.; Anton, A. B.; Apai, G. *J. Am. Chem. Soc.* **1992**, *114*, 4410.
- (14) Celio, H.; Smith, K. C.; White, J. M. *J. Am. Chem. Soc.* **1999**, *121*, 10422.
- (15) Bent, B. E.; Nuzzo, R. G.; Zegarski, B. R.; Dubois, L. H. *J. Am. Chem. Soc.* **1991**, *113*, 1143.
- (16) Scoggins, T. B.; White, J. M. *J. Phys. Chem. B* **1997**, *101*, 7958.
- (17) Chrysostomou, D.; Flowers, J.; Zaera, F. *Surf. Sci.* **1999**, *439*, 34.
- (18) Öfner, H.; Zaera, F. *J. Phys. Chem. B* **1997**, *101*, 9069.
- (19) Hoffmann, H.; Griffiths, P. R.; Zaera, F. *Surf. Sci.* **1992**, *262*, 141.
- (20) Steininger, H.; Lehwald, S.; Ibach, H. *Surf. Sci.* **1982**, *123*, 264.
- (21) Zaera, F. *Surf. Sci.* **1991**, *255*, 280.
- (22) Zhdanov, V. P.; Kasemo, B. *Surf. Sci.* **1998**, *415*, 403.
- (23) Zaera, F. *Langmuir* **1996**, *12*, 88.
- (24) Christmann, K.; Ertl, G.; Pignet, T. *Surf. Sci.* **1976**, *54*, 365.
- (25) McLachlan, R. D.; Nyquist, R. A. *Spectrochim. Acta A* **1968**, *24*, 103.
- (26) Greenler, R. G. *J. Chem. Phys.* **1966**, *44*, 310.
- (27) Zaera, F. In *Encyclopedia of Chemical Physics and Physical Chemistry*; Moore, J. H., Spencer, N. D., Eds.; IOP Publishing Inc.: Philadelphia, in press.
- (28) Zaera, F.; Hoffmann, H.; Griffiths, P. R. *J. Electron Spectrosc. Relat. Phenom.* **1990**, *54/55*, 705.
- (29) French, C.; Zaera, F. *Phys. Rev. Lett.* **1999**, *309*, 321.
- (30) Paliani, G.; Poletti, A.; Cardaci, G.; Murgia, S. M.; Cataliotti, R. *J. Organomet. Chem.* **1973**, *60*, 157.
- (31) Andrews, D. C.; Davidson, G. *J. Organomet. Chem.* **1973**, *55*, 383.
- (32) Zaera, F. *J. Phys. Chem.* **1990**, *94*, 5090.
- (33) Zaera, F.; Bernstein, N. *J. Am. Chem. Soc.* **1994**, *116*, 4881.
- (34) Janssens, T. V. W.; Zaera, F. *Surf. Sci.* **1995**, *344*, 77.
- (35) Zaera, F.; Janssens, T. V. W.; Öfner, H. *Surf. Sci.* **1996**, *368*, 371.
- (36) Öfner, H.; Zaera, F. *J. Phys. Chem.* **1997**, *101*, 396.
- (37) Janssens, T. V. W.; Stone, D.; Hemminger, J. C.; Zaera, F. *J. Catal.* **1998**, *177*, 284.
- (38) Zaera, F. *Isr. J. Chem.* **1998**, *38*, 293.
- (39) Zaera, F.; French, C. R. *J. Am. Chem. Soc.* **1999**, *121*, 2236.